Coefficients optimization and low-complexity equalization for OTFS-RIS system

Rabah Ouchikh, Thierry Chonavel, Abdeldjalil Aïssa-El-Bey, Mustapha Djeddou

Coefficients optimization and low-complexity equalization for OTFS-RIS system

Rabah Ouchikh
Lab Télécommunications
Ecole Militaire Polytechnique
Bordj El-Bahri, Algeria
rabah.ouchikh@emp.mdn.dz

Thierry Chonavel
IMT Atlantique, Lab-STICC,
UMR CNRS 6285, F-29238,
Brest, France
thierry.chonavel@imt-atlantique.fr

Abdeldjalil Aïssa-El-Bey
IMT Atlantique, Lab-STICC,
UMR CNRS 6285, F-29238,
Brest, France
abdeldjalil.aissaelbey@imt-atlantique.fr

Mustapha Djeddou
Electronics Department
National Polytechnic School
Algiers, Algeria
mustapha.djeddou@g.enp.edu.dz

***Abstract*—In high-mobility environments, reconfigurable intelligent surface (RIS)-assisted orthogonal time-frequency space (OTFS) systems can significantly improve system performance in terms of bit-error rate (BER), signal-to-noise ratio (SNR), and capacity. These gains depend on the optimal configuration of the RIS reflection coefficients, which must balance the trade-off between reliability and spectral efficiency. In this work, we formulate a bi-objective optimization problem that simultaneously maximizes capacity and minimizes BER, and we solve it using the non-dominated sorting genetic algorithm (NSGA-II). Simulation results show that the proposed method efficiently captures the trade-off between BER and capacity. For instance, at SNR = 5 dB and $K = 8$ RIS elements, the Pareto front demonstrates that improving the achievable rate inevitably increases BER, while minimizing BER reduces capacity, allowing flexible adaptation depending on the target application (e.g., mission-critical reliability vs. high data rate). Compared with state-of-the-art methods such as the strongest delay-Doppler channel response and Frobenius norm-based optimization, our approach achieves superior BER and capacity performance. Furthermore, we propose a low-complexity equalizer based on QR decomposition with Givens rotations. Complexity analysis shows that, unlike conventional equalizers, the proposed scheme maintains complexity independent of the number of RIS elements K and achieves much better performance when $K > K_{lim}$. Overall, the proposed framework provides an effective solution for enabling reliable and efficient OTFS-RIS systems in 6G high-mobility scenarios.**

***Index Terms*—RIS, OTFS, low-complexity equalization, high-mobility, bi-objective optimization.**

I. Introduction

Recent studies have highlighted the reconfigurable intelligent surface (RIS)-assisted orthogonal time frequency space (OTFS) as a key technology for improving wireless system performance in terms of signal-to-noise ratio (SNR), bit error rate (BER) and capacity for high-mobility scenarios by optimally configuring the RIS reflection coefficients [1]–[5].

In [1], an RIS phase optimization method was proposed, where only the dominant delay-Doppler path was phase-aligned, while non-dominant paths remained misaligned with the direct path. In [2], the RIS phase shifts were designed to maximize the received SNR in both single-input single-output (SISO) and multiple-input multiple-output (MIMO) systems. Furthermore, in [3], the authors optimize the phase vector at the RIS by maximizing the Frobenius norm of the effective end-to-end delay-Doppler channel matrix in the RIS-assisted OTFS system. In [4], the authors selected the phase through random Monte Carlo sampling, aiming to maximize the Frobenius norm of the superimposed channel matrix. It is crucial to note that in the aforementioned studies [1]–[4], the authors did not directly address optimization problems related to capacity or BER. To bridge this gap, the authors in [5] designed the RIS coefficients with the objective of minimizing the BER, solving the optimization problem using a gradient descent-based approach.

Considering that optimizing for a single objective may not be effectively optimal for achieving others, this paper proposes a joint optimization strategy for designing RIS coefficients. Specifically, we optimize both capacity and BER by formulating a bi-objective function in terms of the reflection coefficients and the eigenvalues of the effective delay-Doppler channel matrix. To solve this optimization problem, we employ a non-dominated sorting genetic algorithm (NSGA)-II-based approach. On the other hand, in RIS-based OTFS systems, the high-dimensional nature of the delay-Doppler channel matrix poses computational challenges for conventional linear equalization techniques. To address them, we leverage the block-circulant structure and sparsity of the channel matrix and propose a low-complexity equalizer based on QR decomposition using Givens rotations. Finally, through numerical simulations, we demonstrate the effectiveness of the proposed optimization framework in terms of capacity and BER performance, comparing it with state-of-the-art techniques [1]–[5]. We also conduct computational evaluations of the proposed low-complexity equalizer and compare them with a recent linear equalization method [5].

II. OTFS-RIS system model

We consider an uplink OTFS-RIS system consisting of a single user, a single base station (BS), and one RIS network. The RIS is composed of K reflecting elements, whose reflection coefficients can be dynamically adjusted to enhance performance at the receiver. Both the user and the BS are assumed to be equipped with a single antenna. The user constructs the delay-Doppler matrix $\boldsymbol{X} \in \mathbb{C}^{M \times N}$ by mapping information symbols $x[k, l]$ from a finite alphabet $\mathcal{A}$ (M-QAM or M-PSK). Here, N and M denote the number of Doppler and delay bins, respectively. The OTFS transmitter processes

$\boldsymbol{X}$ by applying an inverse symplectic finite Fourier transform (ISFFT) followed by a Heisenberg transform leading to the time-domain signal:

$$\boldsymbol{S} = \boldsymbol{G}_{tx}\boldsymbol{F}_M^H(\boldsymbol{F}_M\boldsymbol{X}\boldsymbol{F}_N^H) = \boldsymbol{G}_{tx}\boldsymbol{X}\boldsymbol{F}_N^H, \tag{1}$$

where $\boldsymbol{F}_n$ is the $(n \times n)$ discrete Fourier transform (DFT) matrix and $\boldsymbol{G}_{tx} = \text{diag}\{g_{tx}(0), ..., g_{tx}((M-1)T/M)\} \in \mathbb{C}^{M\times M}$, where g_{tx} is the pulse shaping waveform.

With a rectangular waveform as the pulse-shaping function $\boldsymbol{G}_{tx}$ reduces to the identity matrix $\boldsymbol{I}_M$ and the transmitted time-domain signal in its vectorized form is given by

$$\boldsymbol{s} = (\boldsymbol{F}_N^H \otimes \boldsymbol{I}_M)\boldsymbol{x}, \tag{2}$$

where $\boldsymbol{s} = \text{vec}(\boldsymbol{S})$ and $\boldsymbol{x} = \text{vec}(\boldsymbol{X})$.

A single cyclic prefix (CP) is appended to the signal $s(t)$ before transmission to mitigate inter-symbol interference between OTFS blocks.

The signal $\boldsymbol{s}$ is transmitted through a time-varying wireless channel consisting of three links: the user-to-k-th RIS link, the k-th RIS-to-BS link, and the direct user-to-BS link. The delay-Doppler channel impulse responses for the three links are given as follows [6]:

$$\text{user-to-}k\text{-th RIS: } h^{(k)}(\tau,\nu) = \sum_{i=1}^{L_1} h_i^{(k)}\delta(\tau-\tau_{1,i}^{(k)})\delta(\nu-\nu_{1,i}^{(k)}), \tag{3}$$

$$k\text{-th RIS-to-BS: } g^{(k)}(\tau,\nu) = \sum_{i=1}^{L_2} g_i^{(k)}\delta(\tau-\tau_{2,i}^{(k)})\delta(\nu-\nu_{2,i}^{(k)}), \tag{4}$$

$$\text{direct user-to-BS: } h^{(d)}(\tau,\nu) = \sum_{i=1}^{L_d} h_i^{(d)}\delta(\tau-\tau_i)\delta(\nu-\nu_i), \tag{5}$$

where L_1, L_2, and L_d represent the number of paths and $(\tau_{1,i}^{(k)} = \frac{l_{1,i}^{(k)}}{M\Delta f}, \nu_{1,i}^{(k)} = \frac{k_{1,i}^{(k)}}{NT})$, $(\tau_{2,i}^{(r)} = \frac{l_{2,i}^{(k)}}{M\Delta f}, \nu_{2,i}^{(k)} = \frac{k_{2,i}^{(k)}}{NT})$, and $(\tau_i = \frac{l_i}{M\Delta f}, \nu_i = \frac{k_i}{NT})$ denote their corresponding delay and Doppler shifts, with the respective delay and Doppler indices, assumed to be integers, given by $(l_{1,i}^{(k)}, k_{1,i}^{(k)})$, $(l_{2,i}^{(k)}, k_{2,i}^{(k)})$, and (l_i, k_i). Furthermore, the parameters $h_i^{(k)}$, $g_i^{(k)}$, and $h_i^{(d)} \sim \mathcal{CN}(0,1)$ represent the channel coefficients for their respective links.

The received signal at the BS through the k-th reflecting surface can be expressed as

$$\boldsymbol{r}^{(k)} = \phi_k\boldsymbol{H}^{(k)}\boldsymbol{s} + \boldsymbol{n}^{(k)}, \tag{6}$$

where $\phi_k = \alpha_k e^{j\theta_k}$ represents the reflection coefficient of the k-th RIS element, with magnitude $\alpha_k \in [0, \alpha_{k,\max}]$ and phase $\theta_k \in [0, 2\pi]$. $\boldsymbol{H}^{(k)} = \boldsymbol{H}_2^{(k)}\boldsymbol{H}_1^{(k)} \in \mathbb{C}^{MN\times MN}$, where $\boldsymbol{H}_1^{(k)} = \sum_{i=1}^{P_1} h_i^{(k)}\boldsymbol{\Pi}^{l_{1,i}^{(k)}}\boldsymbol{\Delta}^{k_{1,i}^{(k)}}$ and $\boldsymbol{H}_2^{(k)} = \sum_{i=1}^{P_2} g_i^{(k)}\boldsymbol{\Pi}^{l_{2,i}^{(k)}}\boldsymbol{\Delta}^{k_{2,i}^{(k)}}$. $\boldsymbol{\Delta} = \text{diag}\{e^{j2\pi(0)/MN}, e^{j2\pi(1)/MN}, ..., e^{j2\pi(MN-1)/MN}\} \in \mathbb{C}^{MN\times MN}$ and $\boldsymbol{\Pi} \in \mathbb{C}^{MN\times MN}$ with $\boldsymbol{\Pi}_{a,b} = 1$ if $b = a+1$ and 0 otherwise. $\boldsymbol{n}^{(k)}$ is the additive white Gaussian noise (AWGN) vector where $\boldsymbol{n}_i^{(k)} \sim \mathcal{CN}(0, \frac{\sigma_n^2}{K+1})$.

Next, the received signal at the BS through the user-to-BS direct link is given by

$$\boldsymbol{r}^d = \boldsymbol{H}^d\boldsymbol{s} + \boldsymbol{n}^d, \tag{7}$$

where $\boldsymbol{H}^d = \sum_{i=1}^{L_d} h_i^d\boldsymbol{\Pi}^{l_i}\boldsymbol{\Delta}^{k_i}$. Now, the final expression for the received signal at the BS is given by

$$\boldsymbol{r} = \boldsymbol{r}^d + \sum_{k=1}^{K}\boldsymbol{r}^{(k)} = \boldsymbol{H}\boldsymbol{s} + \boldsymbol{n}, \tag{8}$$

where $\boldsymbol{H} = \boldsymbol{H}^d + \sum_{k=1}^{K}\phi_k\boldsymbol{H}^{(k)}$ is the channel matrix and $\boldsymbol{n}$ is the AWGN vector with $n_i \sim \mathcal{CN}(0, \sigma_n^2)$.

The OTFS receiver processes $\boldsymbol{r}$ by applying Wigner transform followed by a symplectic finite Fourier transform (SFFT), leading to the delay-Doppler signal $\boldsymbol{y} \in \mathcal{C}^{MN\times 1}$. Assuming the rectangular waveform as pulse-shaping waveform, $\boldsymbol{y}$ can be expressed as

$$\boldsymbol{y} = (\boldsymbol{F}_N \otimes \boldsymbol{I}_M)\boldsymbol{r}. \tag{9}$$

By substituting (2) into (8) and then (8) into (9), $\boldsymbol{y}$ takes the following form:

$$\boldsymbol{y} = \boldsymbol{H}_{\text{eff}}\boldsymbol{x} + \boldsymbol{w}, \tag{10}$$

where $\boldsymbol{H}_{\text{eff}} = \boldsymbol{H}_{\text{eff}}^{(d)} + \sum_{k=1}^{K}\phi_k\boldsymbol{H}_{\text{eff}}^{(k)}$ is the effective channel matrix with $\boldsymbol{H}_{\text{eff}}^{(u)} = (\boldsymbol{F}_N \otimes \boldsymbol{I}_M)\boldsymbol{H}^{(u)}(\boldsymbol{F}_N^H \otimes \boldsymbol{I}_M)$, for $u \in \{1 : k, d\}$ and $\boldsymbol{w} = (\boldsymbol{F}_N \otimes \boldsymbol{I}_M)\boldsymbol{n}$. Since $(\boldsymbol{F}_N \otimes \boldsymbol{I}_M)$ is a unitary matrix and the entries of $\boldsymbol{n}$ are i.i.d, $\boldsymbol{w}$ and $\boldsymbol{n}$ follow the same distribution.

III. Proposed coefficients optimization problem

A. Capacity maximization

As in an OTFS system, the capacity of an OTFS-RIS system is given by [1]:

$$C = \frac{1}{MN}\log_2\left|\boldsymbol{I}_{MN} + \frac{P_t\boldsymbol{H}_{\text{eff}}^H\boldsymbol{H}_{\text{eff}}}{\sigma_n^2 NM}\right|, \tag{11}$$

where P_t is the transmit power.

To simplify Equation (11), we use the following eigen-value-decomposition of $\boldsymbol{H}_{\text{eff}}^{(u)}$: $\boldsymbol{H}_{\text{eff}}^{(u)} = \boldsymbol{V}\boldsymbol{\Lambda}^{(u)}\boldsymbol{V}^H$, where $\boldsymbol{V} = (\boldsymbol{F}_N \otimes \boldsymbol{F}_M)^H$ and $\boldsymbol{\Lambda}^{(u)} = \text{diag}\{\lambda_1^{(u)}, \lambda_2^{(u)}, ..., \lambda_{MN}^{(u)}\}$ with $\lambda_i^{(u)}$ the i-th eigen-value of $\boldsymbol{H}_{\text{eff}}^{(u)}$, $(u \in \{1 : K, d\})$.

Then, from (11),

$$\boldsymbol{H}_{\text{eff}} = \boldsymbol{V}\left(\boldsymbol{\Lambda}^{(d)} + \sum_{k=1}^{K}\phi_k\boldsymbol{\Lambda}^{(k)}\right)\boldsymbol{V}^H. \tag{12}$$

Substituting (12) in (11), the capacity expression can be simplified as

$$C = \frac{1}{MN}\sum_{i=1}^{MN}\log_2\left(1 + \frac{\gamma}{MN}|\lambda_i|^2\right), \tag{13}$$

where $\gamma = \frac{P_t}{\sigma_n^2}$ is the SNR and $\lambda_i = \lambda_i^{(d)} + \sum_{k=1}^{K} \phi_k \lambda_i^{(k)}$.

To maximize the capacity with respect to the reflection coefficients vector $\boldsymbol{\phi} = [\phi_1, \phi_2, ..., \phi_K]$, we should solve the following optimization problem:

$$\begin{aligned} \max_{\boldsymbol{\phi}} \quad & \sum_{i=1}^{MN} \log_2 \left(1 + \frac{\gamma}{MN} |\lambda_i|^2\right) \\ \text{s.t.} \quad & \lambda_i = \lambda_i^{(d)} + \sum_{k=1}^{K} \alpha_k e^{i\theta_k} \lambda_i^{(k)}, i = 1 : MN, \\ & 0 \le \alpha_k \le \alpha_{k,\max}, \quad \forall k \in \{1, \ldots, K\}, \\ & 0 \le \theta_k \le 2\pi, \quad \forall k \in \{1, \ldots, K\}. \end{aligned} \tag{P1}$$

B. BER minimization

Given the received signal $\boldsymbol{y}$, the LMMSE equalized symbols are obtained as: $\hat{\boldsymbol{x}}_{\text{MMSE}} = (\boldsymbol{H}_{\text{eff}}^H \boldsymbol{H}_{\text{eff}} + \sigma_n^2 \boldsymbol{I}_{MN})^{-1} \boldsymbol{H}_{\text{eff}}^H \boldsymbol{y}$. To minimize the BER, it is necessary to maximize the signal to interference plus noise ratio (SINR), whose instantaneous expression of the j-th equalized symbol is given by

$$\gamma_j = \frac{\gamma MN}{\sum_{i=1}^{MN} (\sigma_n^2 + |\lambda_i|^2)^{-1}} - 1. \tag{14}$$

Following a similar approach to [5], the BER minimization can be formulated as:

$$\begin{aligned} \min_{\boldsymbol{\phi}} \quad & \sum_{i=1}^{MN} (\sigma_n^2 + |\lambda_i|^2)^{-1} \\ \text{s.t.} \quad & \lambda_i = \lambda_i^{(d)} + \sum_{k=1}^{K} \alpha_k e^{i\theta_k} \lambda_i^{(k)}, i = 1 : MN, \\ & 0 \le \alpha_k \le \alpha_{k,\max}, \quad \forall k \in \{1, \ldots, K\}, \\ & 0 \le \theta_k \le 2\pi, \quad \forall k \in \{1, \ldots, K\}. \end{aligned} \tag{P2}$$

C. Joint capacity and BER optimization

The objective here is to determine the optimal RIS coefficients that maximize capacity while minimizing BER. From a fundamental communication theory perspective, capacity and BER inherently impose constraints on each other; enhancing capacity may lead to an increase in BER, and vice versa. Therefore, in this section, we aim to find a trade-off between these two performance metrics. To achieve this, we formulate the following bi-objective optimization problem obtained by considering the optimization problems (P1) and (P2):

$$\begin{aligned} \min_{\boldsymbol{\phi}} \quad & -\sum_{i=1}^{MN} \log_2 \left(1 + \frac{\gamma}{MN} |\lambda_i|^2\right) \\ \min_{\boldsymbol{\phi}} \quad & \sum_{i=1}^{MN} (\sigma_n^2 + |\lambda_i|^2)^{-1} \\ \text{s.t.} \quad & \lambda_i = \lambda_i^{(d)} + \sum_{k=1}^{K} \alpha_k e^{i\theta_k} \lambda_i^{(k)}, i = 1 : MN, \\ & 0 \le \alpha_k \le \alpha_{k,\max}, \quad \forall k \in \{1, \ldots, K\}, \\ & 0 \le \theta_k \le 2\pi, \quad \forall k \in \{1, \ldots, K\}. \end{aligned} \tag{P3}$$

To solve the optimization problem (P3), we employed the non-dominated sorting genetic algorithm II (NSGA-II) [7]. This multi-objective optimization algorithm enables the simultaneous optimization of capacity and BER while maintaining a balance between these two criteria. By leveraging its dominance-based sorting and diversity-preserving mechanisms, NSGA-II efficiently explores the solution space, leading to optimal RIS coefficients that enhance the performance of the OTFS-RIS system. Considering $f_1 = -\sum_{i=1}^{MN} \log_2 \left(1 + \frac{\gamma}{MN} |\lambda_i|^2\right)$ and $f_2 = \sum_{i=1}^{MN} (\sigma_n^2 + |\lambda_i|^2)^{-1}$, the NSGA-II algorithm starts by generating an initial population and evaluating f_1 and f_2. The solutions are then ranked through non-dominated sorting, organizing them into Pareto fronts, with the first front containing the most optimal solutions. To ensure diversity, a crowding distance measure is applied. Selection is carried out using a Pareto-based tournament, favoring solutions that exhibit both dominance and diversity. Genetic operators, such as crossover and mutation, generate new candidate solutions, and the population is updated by merging parents and offspring while keeping the best individuals. This iterative process continues until the Pareto front stabilizes between successive generations or a predefined number of iterations N_{iter} is reached. The final set of Pareto-optimal solutions represents the values of $\boldsymbol{\Phi}$ that achieve the best trade-off between capacity and BER. The detailed steps of the proposed optimization procedure are summarized in Algorithm 1.

IV. Proposed low-complexity equalizer

In the OTFS-RIS system, the linear minimum mean square error (LMMSE) equalized symbols can be computed from the received signal $\boldsymbol{y}$ in (10) as $\hat{\boldsymbol{x}} = \boldsymbol{W}_{\text{MMSE}} \boldsymbol{y}$, where

$$\boldsymbol{W}_{\text{MMSE}} = \left(\boldsymbol{H}_{\text{eff}}^H \boldsymbol{H}_{\text{eff}} + \sigma_n^2 \boldsymbol{I}_{MN}\right)^{-1} \boldsymbol{H}_{\text{eff}}^H. \tag{15}$$

However, this equalization process requires the inversion of an $MN \times MN$ matrix, resulting in a high computational complexity of $\mathcal{O}((MN)^3)$. Therefore, we propose a low-complexity equalizer that leverage the sparsity and block-circulant structure of $\boldsymbol{H}_{\text{eff}}$. The proposed equalizer is based on QR decomposition using Givens rotations.

The matrix $\boldsymbol{H}_{\text{eff}}$ is a block circulant matrix, composed of two matrices: $\boldsymbol{H}_{\text{eff}}^{(\text{d})}$, which has exactly L_d non-zero elements per row and column, and $\boldsymbol{H}_{\text{eff}}^{\text{ind}} = \sum_{i=1}^{K} \phi_k \boldsymbol{H}_{\text{eff}}^{(k)}$, which contains $L_1 + L_2 - 1$ non-zero elements per row and column. Note that $\boldsymbol{H}_{\text{eff}}$ has $L \le L_1 + L_2 + L_d - 1$ non-zero elements in each row and column and less if common paths exist between the direct and RIS-assisted links. Let $L = L_l + L_h$, where L_l is the number of non-zero elements below the diagonal, and L_h is the number of non-zero elements in the remaining positions of $\boldsymbol{H}_{\text{eff}}$.

Our objective is to determine the transmitted symbols vector $\boldsymbol{x}$ in a computationally efficient manner while taking advantage of the sparsity of $\boldsymbol{H}_{\text{eff}}$ discussed in the previous paragraph. Our approach involves using Givens rotations to eliminate the non-zero elements below the diagonal, transforming $\boldsymbol{H}_{\text{eff}}$ into

Algorithm 1 Proposed NSGA-II algorithm for solving (P3)

Input: Population size P, number of generations N_{iter}, RIS elements K

Output: Pareto-optimal reflection coefficients $\mathbf{\Phi}^*$

Initialize population Pop with P random RIS coefficient vectors $\boldsymbol{\phi}^{(i)} = [\phi_1, \ldots, \phi_K]$, $i = 1 : P$

Set $g \leftarrow 0$

while Pareto front not stabilized **and** $g < N_{iter}$ **do**

Step 1: Objective evaluation

- Evaluate objectives $f_1(\boldsymbol{\phi}^{(i)})$ and $f_2(\boldsymbol{\phi}^{(i)})$ for each solution $\boldsymbol{\phi}^{(i)} \in Pop$

Step 2: Non-dominated sorting

- Compare all solutions pairwise.
- Solution A dominates B if A is no worse than B in all objectives and strictly better in at least one.
- Organize individuals into Pareto fronts: Front 1 = non-dominated set, Front 2 = dominated only by Front 1, etc.

Step 3: Diversity preservation (Crowding distance)

- For each front, compute a crowding distance for every solution.
- For each objective, sort individuals and assign large distance to boundary solutions.
- For intermediate solutions, distance = normalized difference of adjacent objective values.
- Ensures spread of solutions across the Pareto front.

Step 4: Selection (Tournament)

- Randomly pick two candidates from the population.
- Choose the one with lower Pareto rank (better front).
- If both have the same rank, select the one with larger crowding distance.
- Repeat until enough parents are chosen.

Step 5: Variation (Crossover and Mutation)

- Apply simulated binary crossover (SBX) to generate offspring from selected parents.
- Apply polynomial mutation (or Gaussian) to slightly perturb RIS coefficients.
- This introduces exploration while preserving feasibility of constraints.

Step 6: Population update

- Merge parents and offspring into a combined population of size $2P$.
- Sort the combined set using non-dominated sorting.
- Fill the next generation by selecting complete Pareto fronts in order.
- If the last front exceeds the capacity, choose individuals with the largest crowding distance.
- Keep exactly P solutions for the next generation.

end while

$g \leftarrow g + 1$

Return $\mathbf{\Phi}^*$, the optimal trade-off between C and BER.

an upper triangular matrix $\boldsymbol{R}$, and then solving the resulting system $\boldsymbol{R}\boldsymbol{x} = \boldsymbol{Q}^H\boldsymbol{y}$, where $\boldsymbol{Q}$ is a unitary matrix and $\boldsymbol{R}$ is an upper triangular matrix.

The Givens rotation technique eliminates a specific element of a matrix at a time by applying a two-dimensional rotation transformations. Consequently, the rotation matrix significantly impacts the performance of QR decomposition. Consider a 4×4 complex-valued matrix

$$\boldsymbol{H} = \begin{bmatrix} |h_{11}|e^{j\theta_{11}} & h_{12} & h_{13} & h_{14} \\ |h_{21}|e^{j\theta_{21}} & h_{22} & h_{23} & h_{24} \\ h_{31} & h_{32} & h_{33} & h_{34} \\ h_{41} & h_{42} & h_{43} & h_{44} \end{bmatrix},$$

where $|h_{i1}|$ and θ_{i1} $(i = 1, 2)$ denote, respectively, the magnitude and the angle of the matrix entries.

The first Givens rotation matrix, $\boldsymbol{G}_1$, is designed to eliminate h_{21} using h_{11} and can be represented as follows:

$$\boldsymbol{G}_1 = \begin{bmatrix} c & s & 0 & 0 \\ -s^* & c^* & 0 & 0 \\ 0 & 0 & 1 & 0 \\ 0 & 0 & 0 & 1 \end{bmatrix}.$$

The complex upper triangular matrix $\boldsymbol{R}$ and the complex unitary matrix $\boldsymbol{Q}$ are determined as follows:

$$\begin{aligned} \boldsymbol{R} &= \boldsymbol{G}_6\boldsymbol{G}_5\boldsymbol{G}_4\boldsymbol{G}_3\boldsymbol{G}_2\boldsymbol{G}_1, \\ \boldsymbol{Q} &= (\boldsymbol{G}_6\boldsymbol{G}_5\boldsymbol{G}_4\boldsymbol{G}_3\boldsymbol{G}_2\boldsymbol{G}_1)^H, \end{aligned} \tag{16}$$

where $\boldsymbol{G}_2$, ..., $\boldsymbol{G}_6$ denote rotation matrices to zero h_{31}, h_{41}, h_{32}, h_{42} and h_{43}, respectively.

The parameters c and s can be determined using the two-angle complex rotation (Two-ACR) technique, as follows:

$$\begin{aligned} c &= \frac{|h_{11}|}{\sqrt{|h_{11}|^2 + |h_{21}|^2}} = \cos(\theta_a), \\ s &= \frac{|h_{21}|e^{j\phi_b}}{\sqrt{|h_{11}|^2 + |h_{21}|^2}} = \sin(\theta_a)e^{(\theta_b)}, \end{aligned} \tag{17}$$

where $\theta_b = \theta_{11} - \theta_{21}$ and $\theta_a = \arctan\left(\frac{|h_{21}|}{|h_{11}|}\right)$.

Applying this procedure to system (10) and considering that the matrix $\boldsymbol{H}_{\text{eff}}$ has L_l non-zero elements below the diagonal, we obtain the following system:

$$\boldsymbol{Q}^H\boldsymbol{y} = \boldsymbol{R}\boldsymbol{x} + \tilde{\boldsymbol{w}}, \tag{18}$$

where $\tilde{\boldsymbol{w}} = \boldsymbol{Q}^H\boldsymbol{w}$, $\boldsymbol{R} = \boldsymbol{G}_{P_t} \times ... \times \boldsymbol{G}_1$, and $\boldsymbol{Q} = (\boldsymbol{G}_{P_t} \times ... \times \boldsymbol{G}_1)^H$.

Then, to obtain $\boldsymbol{x}$, we solve the system (18) using back-substitution.

V. Complexity analysis

In this section, we analyze the complexity of the proposed equalizer in terms of complex multiplications (CMs). The proposed algorithm consists of two main steps. The first step involves eliminating the elements below the diagonal of $\boldsymbol{H}_{\text{eff}}$ by computing the product $\boldsymbol{Q}^H\boldsymbol{y}$, requiring $\mathcal{O}(L_lMN)$ CMs.

TABLE I: Parameter of the delay-Doppler channel.

Number of channel tap	1	2	3	4	5
Doppler shift (kHz)	0	0.47	0.94	1.41	1.88
delay shift (μs)	0	2.08	4.164	6.246	8.328
Path power (dB)	1	-1.804	-3.565	-5.376	-8.86

The second step recovers the data symbol vector $\boldsymbol{x}$ through back-substitution by solving an upper triangular system. Due to the cyclic nature of $\boldsymbol{H}_{\text{eff}}$, even after its transformation into an upper triangular matrix, it retains $L_h - MN - S$ zero elements, reducing the back-substitution complexity to $\mathcal{O}(S + MN)$ instead of $\mathcal{O}((MN)^2)$, where S represents the number of non-zero elements, with $S << \frac{(MN)^2}{2}$. Thus, the complexity of back-substitution becomes $\mathcal{O}(MN)$ for large values of MN. Consequently, the total complexity of the proposed algorithm is $\mathcal{O}((L_l + 1)MN)$. It is worth noting that the complexity of our proposed algorithm is independent of the number of RIS elements K.

VI. Simulation results

In this section, we present the simulation results of our proposed solution in terms of BER, capacity, and computational complexity. We compare our approach with state-of-the-art methods to highlight its advantages.

For our simulations, we consider an OTFS-RIS system where each OTFS frame consists of $M = 32$ delay bins and $N = 32$ Doppler bins, with a carrier frequency of $f_c = 4$ GHz and a sub-carrier spacing of $\Delta f = 15$ kHz. The delay-Doppler symbols are modulated using QPSK constellation. As in [5], the delay-Doppler channel parameters, summarized in Table I, are assigned as follows: the first 3 taps correspond to the user-to-RIS link, the first 4 taps to the RIS-to-BS link, and the 5 taps to the user-to-BS direct link.

Figure 1 illustrates the Pareto front obtained by solving problem (P3) using the NSGA-II algorithm for $K = 8$ RIS elements at an SNR of 5 dB. Each point on the curve represents a trade-off solution between maximizing capacity and minimizing BER. As expected, improving the capacity comes at the expense of higher BER, while minimizing BER reduces the achievable rate. This demonstrates the effectiveness of the proposed NSGA-II approach in capturing the inherent trade-off between reliability and spectral efficiency in RIS-assisted OTFS systems. The choice of the operating point along the Pareto front therefore depends on the requirements of the target application, e.g., prioritizing reliability for mission-critical communications or maximizing throughput for high-data-rate services.

Figure 2 shows the BER and capacity performance as a function of SNR for different RIS configurations. We solve the optimization problems (P1), (P2), and (P3) using the suggested NSGA-II algorithm with $K \in \{4, 8\}$. In Figure 2a, the BER performance is evaluated using the proposed equalizer, while in Figure 2b, the capacity is computed using equation (13). We denote by $\boldsymbol{\Phi}_{P_1}$ and $\boldsymbol{\Phi}_{P_2}$ the optimal solutions to problems

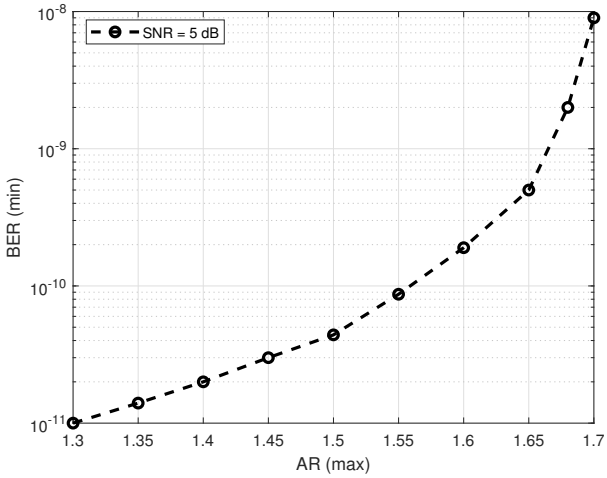

Fig. 1: Pareto front obtained by the proposed NSGA-II algorithm for problem (P3) for $K = 8$ and SNR $= 5$ dB.

(P1) and (P2), respectively. Additionally, $\boldsymbol{\Phi}_{P_3}^{(i)}$ represents the i-th optimal solution belonging to the Pareto front obtained by solving Problem (P3). From Figure 2a, it is shown that $\boldsymbol{\Phi}_{P_2}$ minimizes the BER; however, as observed in Figure 2b, it does not maximize capacity. Similarly, while $\boldsymbol{\Phi}_{P_1}$ maximizes capacity, it fails to minimize the BER. These figures further illustrate that considering the proposed solution for the joint optimization of BER and capacity ($\boldsymbol{\Phi}_{P_3}^{(i)}$) enables an effective trade-off between these two performance metrics. Moreover, the results indicate that the proposed solution outperforms state-of-the-art methods, namely strongest delay-Doppler channel response (SDDCR) in [1], [2] and Frobenius norm approach (FN) in [3], [4], in terms of jointly optimizing BER and capacity.

Figure 3 illustrates the computational complexity, in terms of CMs, of the proposed equalizer as a function of the number of subcarriers M for different values of the number of RIS elements $K \in \{2^4, 2^5, 2^6, 2^7, 2^8\}$, We consider a maximum velocity of 250 km/h. In low-latency communication systems, the number of sub-carriers M is significantly larger than the number of Doppler bins N. In this simulation, we set $N = 32$. This figure also presents the computational complexity of the equalizer from [5], given by $\mathcal{O}(MN(L_d + (1 + L_1L_2)K + \log_2(MN))$. From this figure, it can be observed that for small values of K, the computational complexity of the proposed equalizer is higher than that of the existing equalizer in [5]. For instance, when $K = 16$, the complexity of the proposed algorithm is five times greater than that of the existing equalizer for $M = 5000$. However, as K increases, the complexity of the existing equalizer continues to grow until it reaches the complexity of the proposed equalizer at a critical threshold $K = K_{lim} = \frac{L_l+1-L_d-\log_2(MN)}{1+L_1L_2}$. Finally, we can notice that the performance of the proposed equalizer is much better than that of the existing one if the condition $K > K_{lim}$ is satisfied. This phenomenon is justified by the fact that the complexity of the proposed equalizer remains independent of

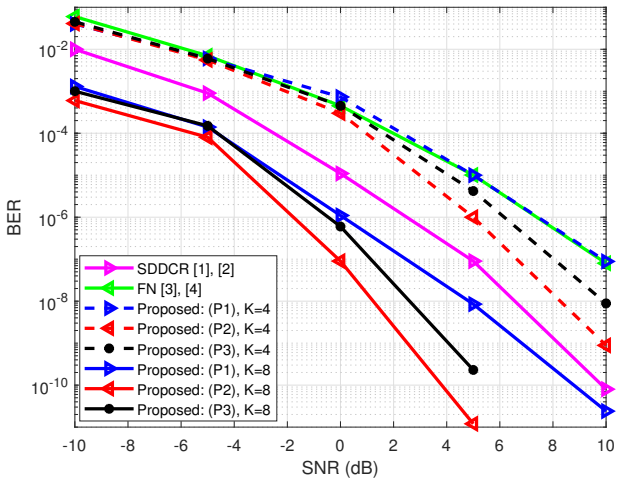

(a) BER performance.

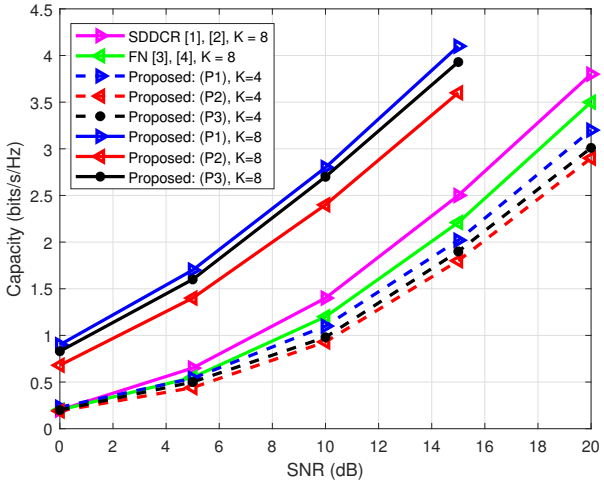

(b) Capacity performance.

Fig. 2: BER and capacity performance of the proposed and state-of-the-art optimization techniques for RIS coefficients.

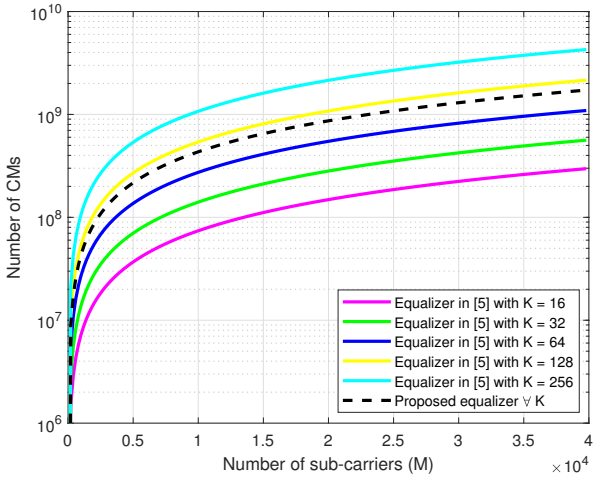

Fig. 3: Computational complexity comparison of the proposed and state-of-the-art equalizer.

K, whereas the complexity of the existing equalizer increases with MNL_1L_2K.

VII. Conclusion

In this paper, we proposed a joint optimization framework for RIS-assisted OTFS systems that simultaneously maximizes capacity and minimizes BER. By formulating a bi-objective optimization problem and solving it using the NSGA-II algorithm, we effectively captured the trade-off between spectral efficiency and reliability. Additionally, we designed a low-complexity equalizer based on QR decomposition with Givens rotations to mitigate the computational challenges associated with high-dimensional delay-Doppler matrices. Simulation results demonstrated the superiority of our approach over existing methods in terms of capacity, BER, and computational efficiency. These findings highlight the potential of jointly optimizing RIS reflection coefficients and employing efficient equalization techniques to enhance OTFS performance in high-mobility environments. This work assumes perfect CSI, which may limit applicability in more practical scenarios. Future work will focus on extending the framework to imperfect CSI, and large-scale MIMO implementations.

References

[1] A. Thomas, K. Deka, S. Sharma, and N. Rajamohan, "IRS-assisted OTFS system: Design and analysis," *IEEE Transactions on Vehicular Technology*, vol. 72, no. 3, pp. 3345–3358, 2022.

[2] A. S. Bora, K. T. Phan, and Y. Hong, "IRS-assisted high mobility communications using OTFS modulation," *IEEE Wireless Communications Letters*, vol. 12, no. 2, pp. 376–380, 2022.

[3] G. Harshavardhan, V. S. Bhat, and A. Chockalingam, "RIS-aided OTFS modulation in high-doppler channels," in *2022 IEEE 33rd Annual International Symposium on Personal, Indoor and Mobile Radio Communications (PIMRC)*, pp. 409–415, 2022.

[4] V. S. Bhat, G. Harshavardhan, and A. Chockalingam, "Input-output relation and performance of RIS-aided OTFS with fractional delay-doppler," *IEEE Communications Letters*, vol. 27, no. 1, pp. 337–341, 2022.

[5] R. K. Yadav, H. B. Mishra, S. Mukhopadhyay, and R. Mishra, "IRS-OTFS systems: Design of reflection coefficients for low-complexity ZF equalizer," *IEEE Transactions on Vehicular Technology*, 2024.

[6] R. Ouchikh, T. Chonavel, A. Aïssa-El-Bey, and M. Djeddou, "Joint channel estimation and data detection for high rate orthogonal time frequency space systems," *International Journal of Communication Systems*, vol. 36, no. 16, p. e5579, 2023.

[7] K. Deb, A. Pratap, S. Agarwal, and T. Meyarivan, "A fast and elitist multiobjective genetic algorithm: NSGA-II," *IEEE transactions on evolutionary computation*, vol. 6, no. 2, pp. 182–197, 2002.